

Dynamics of 8-Oxoguanine in DNA: Decisive Effects of Base Pairing and Nucleotide Context

Sergey S. Ovcharenko, Andrey V. Shernyukov, Dmitry M. Nasonov, Anton V. Endutkin, Dmitry O. Zharkov,* and Elena G. Bagryanskaya*



Cite This: *J. Am. Chem. Soc.* 2023, 145, 5613–5617



Read Online

ACCESS |



Metrics & More



Article Recommendations



Supporting Information

ABSTRACT: 8-Oxo-7,8-dihydroguanine (oxoG), an abundant DNA lesion, can mispair with adenine and induce mutations. To prevent this, cells possess DNA repair glycosylases that excise either oxoG from oxoG:C pairs (bacterial Fpg, human OGG1) or A from oxoG:A mispairs (bacterial MutY, human MUTYH). Early lesion recognition steps remain murky and may include enforced base pair opening or capture of a spontaneously opened pair. We adapted the CLEANEX-PM NMR protocol to detect DNA imino proton exchange and analyzed the dynamics of oxoG:C, oxoG:A, and their undamaged counterparts in nucleotide contexts with different stacking energy. Even in a poorly stacking context, the oxoG:C pair did not open easier than G:C, arguing against extrahelical base capture by Fpg/OGG1. On the contrary, oxoG opposite A significantly populated the extrahelical state, which may assist recognition by MutY/MUTYH.

8-Oxo-7,8-dihydroguanine (oxoG) is a prominent DNA oxidation product (Figure 1).^{1,2} In human cells, the back-

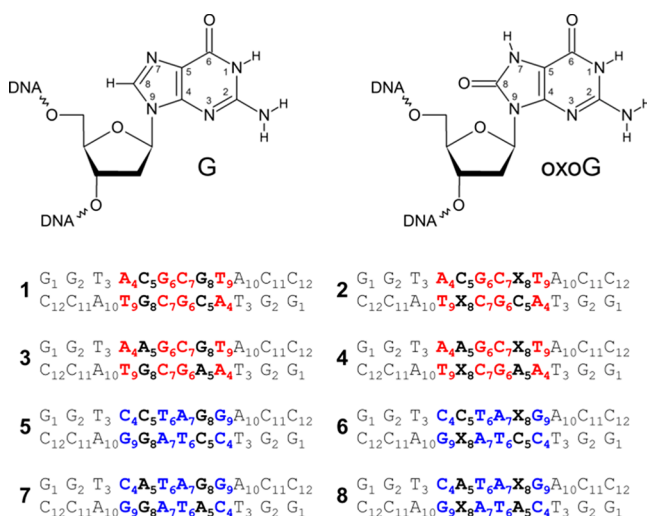


Figure 1. Structures of G and oxoG (X) and the duplexes used in this study. (red) Nucleotides forming a poorly stacking context. (blue) Favorably stacking nucleotides.

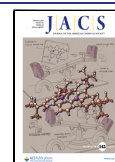
ground oxoG level is $\sim 1/10^6$ guanines, increasing upon oxidative stress.^{2,3} DNA polymerases often incorporate dAMP opposite oxoG producing G:C \rightarrow T:A transversions⁴ that dominate SBS18 and SBS36 cancer mutation signatures.⁵ OxoG prefers the *syn* orientation due to the steric repulsion between O⁸ and deoxyribose.⁶ Base pairing with C stabilizes oxoG in *anti*,⁷ with the clash alleviated by the sugar–phosphate backbone adjustment from BI to BII conformation.⁸ However, upon rotation around the glycosidic bond, oxoG forms a Hoogsteen oxoG(*syn*):A(*anti*) pair^{6,9} (Supporting Information

Figure S1). In contrast, G:A mispairs are intrinsically flexible, accepting both G(*anti*):A(*anti*) and G(*anti*):A(*syn*) conformations.^{10,11} Molecular dynamics simulations show that oxoG mispaired with A flips spontaneously from *anti* to *syn* but remains *anti* opposite to C.¹² Accordingly, the introduction of an 8-oxo group thermodynamically destabilizes the G:C pair but stabilizes the G:A mispair.¹³ The presence of oxoG facilitates DNA bending¹⁴ but increases its torsional rigidity.¹⁵

The mutagenicity of oxoG is countered by DNA repair glycosylases, such as human OGG1 or bacterial Fpg, which excise oxoG from DNA.¹⁶ Despite their common specificity, OGG1 and Fpg are based on different structural folds.^{17,18} Other glycosylases, bacterial MutY and human MUTYH, excise A from oxoG:A, initiating a repair cycle that reinstalls a G:C pair.¹⁶ To avoid mutations, Fpg/OGG1 must selectively recognize oxoG:C but not oxoG:A, whereas MutY/MUTYH recognizes oxoG:A but not oxoG:C. A problem still unsolved is whether these proteins share some common oxoG recognition mechanism. Structural, kinetic, and computational data suggest that oxoG discrimination from G starts when the enzyme encounters the damaged base pair and everts oxoG into an extrahelical pocket.^{17,19,20} Lower stability of the damaged pair may be a major factor early in the recognition, and Fpg was suggested to buckle the oxoG:C pair to facilitate its opening.^{20,21} However, a rival model was proposed for another glycosylase, UNG, which removes uracil from DNA. NMR measurements of base pair opening and closing rates showed

Received: October 24, 2022

Published: March 2, 2023



that UNG delays closing but does not affect opening, suggesting that U is captured in spontaneously opened base pairs.^{22–24}

Despite the potential importance of base pair dynamics for oxoG recognition, experimental information about this lesion is limited. Imino proton exchange measurements indicate that the opening rates and extrahelical lifetimes of oxoG:C and G:C pairs are similar and are ~ 2 orders of magnitude lower than for U:A.^{25,26} However, the dynamics of oxoG:A and the influence of the nucleotide context on the oxoG dynamics remain unstudied.

Base pair opening and closing rates can be estimated using transfer of magnetization from water to measure imino proton exchange (Supporting Information Text), with a caveat that the exchange can already occur at $\sim 30^\circ$ base eversion so the open state is not necessarily fully extrahelical.²⁷ This technique permits determination of exchange rate constants in the range common for imino protons in double-stranded DNA. Among several approaches to transfer of magnetization from water (WEX,²⁸ WEX II,²⁹ MEXICO,³⁰ 2D NOESY/EXSY,³¹ etc.), the CLEAN chemical exchange (CLEANEX-PM)³² is popular when following protein amide protons due to its superior ability to suppress artifacts associated with intramolecular nuclear Overhauser effects (NOEs). Here we have modified the CLEANEX-PM protocol to detect DNA imino proton exchange (Supporting Information Text, Supporting Information Figures S2–S7) and applied it to investigate the dynamics of oxoG:C and oxoG:A. As base pair opening is influenced by stacking with the neighboring pairs,³³ we have designed duplexes based on known G stacking energies,³⁴ placing G or oxoG into poorly stacking C[G/oxoG]T or well-stacking A[G/oxoG]G contexts. The target base was in position 8 of a self-complementary 12-mer (Figure 1) to minimize end effects.⁸

The exchange rate constant k_{ex} relates to the base pair opening and closing rate constants k_{op} and k_{cl} as

$$k_{\text{ex}} = \frac{k_{\text{op}}\alpha(k_0 + k_{\text{B}}[\text{B}])}{k_{\text{cl}} + \alpha(k_0 + k_{\text{B}}[\text{B}])} \quad (1)$$

where k_{B} is the rate constant of proton transfer from an isolated nucleotide to an acceptor (exchange catalyst) B, αk_0 is the exchange rate constant from an open pair without the catalyst, and α accounts for the difference between an isolated nucleotide and an open pair.³⁵ As an exchange catalyst, we chose 2,2-difluoroethylamine (DFEA), which ionizes at physiological pH ($\text{p}K_{\text{a}} = 7.45$ at 25°C) and proved useful in NMR measurements of base pair dynamics.²² If $k_{\text{cl}} \gg \alpha(k_0 + k_{\text{B}}[\text{B}])$ (the EX2 regime, e.g., at low [B]), then

$$k_{\text{ex}} = \frac{k_{\text{op}}\alpha(k_0 + k_{\text{B}}[\text{B}])}{k_{\text{cl}}} = K'_{\text{eq}} \times (k_0 + k_{\text{B}}[\text{B}]) \quad (2)$$

where the apparent equilibrium constant $K'_{\text{eq}} = \alpha K_{\text{eq}} = \alpha k_{\text{op}}/k_{\text{cl}}$ can be extracted as a fitting parameter. If, on the contrary, $k_{\text{cl}} \ll \alpha(k_0 + k_{\text{B}}[\text{B}])$ (as at high [B]), the apparent exchange rate achieves its upper limit $k_{\text{ex}} = k_{\text{op}}$, and an exchange occurs at each base pair opening event. Between these limits, one can establish k_{op} , the apparent closing rate constant $k'_{\text{cl}} = k_{\text{cl}}/\alpha = k_{\text{op}}/K'_{\text{eq}}$ and K'_{eq} .

To follow base pair dynamics, we determined k_{ex} at different DFEA concentrations at 10°C (Figure 2, Supporting Information Figures S8–S11). The data were fitted by eqs 1 or 2 to extract k_{op} and K'_{eq} and calculate k'_{cl} (Table 1, Supporting Information Table S1).

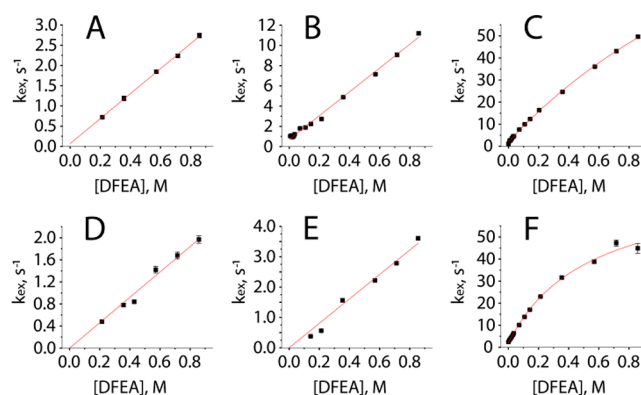


Figure 2. Dependence of k_{ex} on DFEA concentration for G_8 and $\text{oxo}G_8$ in duplexes 1 (A), 2 (B), 4 (C), 5 (D), 6 (E), and 8 (F). Lines show data fitting by eqs 1 (C, F) or 2 (A, B, D, E).

In the Watson–Crick pairs (G:C, oxoG:C; duplexes 1, 2, 5, 6) we followed the exchange of N1 imino protons. OxoG N7 imino proton, exposed to the DNA major groove, was observed as a separate signal at ~ 10 ppm only in the C[oxoG]T context without DFEA, and it was missing in the A[oxoG]G context presumably due to the fast exchange with water protons. Both G:C and oxoG:C pairs demonstrated the EX2 regime with closing much faster than the exchange. Hence, only the apparent equilibrium constants could be compared. In the poorly stacking C[G/oxoG]T context, oxoG was slightly more stable intrahelically ($K'_{\text{eq}} = 0.141 \times 10^{-6}$ for oxoG vs 0.158×10^{-6} for G). In the well-stacking A[G/oxoG]G context, both G and oxoG were even less exposed, and the difference between them widened ($K'_{\text{eq}} = 0.048 \times 10^{-6}$ for oxoG vs 0.118×10^{-6} for G). Thus, even if oxoG:C pairs destabilize the duplex thermodynamically, this is not due to their easier opening. Our equilibrium constants are similar to those reported for the A[G/oxoG]T context by Every and Russu²⁵ (0.21×10^{-6} for oxoG, 0.31×10^{-6} for G). Interestingly, in that work rate constants could be recovered, likely due to the different catalyst employed (NH_3), and were similar for oxoG ($k_{\text{op}} = 38 \text{ s}^{-1}$, $k'_{\text{cl}} = 18 \times 10^7 \text{ s}^{-1}$) and G ($k_{\text{op}} = 47 \text{ s}^{-1}$, $k'_{\text{cl}} = 15 \times 10^7 \text{ s}^{-1}$). Crenshaw et al. measured somewhat higher equilibrium constants (1.6×10^{-6} for oxoG, 1.8×10^{-6} for G) in the A[G/oxoG]A context with a glycine catalyst but were also unable to extract k_{op} and k'_{cl} .²⁵

The situation changed drastically in the adenine-containing mispairs. G_8 N1 imino protons in G:A duplexes 3 and 7 were not observed presumably due to their high solvent accessibility and fast exchange. The only measurable N1/N3 imino protons belonged to G_6 in duplex 3 and to G_2 , T_3 , and G_9 in 7 (Supporting Information Figures S9, S11, Supporting Information Table S1). In contrast, oxoG N7 imino protons engaged in Hoogsteen base pairing were well-resolved. OxoG:A-containing duplexes 4 and 8 showed a kinetic regime that allowed extraction of both k_{op} and k'_{cl} (Table 1). The opening rate constant was expectedly higher for the poorly stacking context (~ 2.4 -fold). Surprisingly, closing also accelerated ~ 4.6 -fold in the C[oxoG]T context, making oxoG overall 1.9-fold more stable intrahelically than in A[oxoG]G. Conceivably, base pair opening could allow the flanking A and G to stack across the gap and keep oxoG from retracting into the helix. Compared with oxoG:C, the equilibrium is shifted by 3–4 orders of magnitude toward the open state in the oxoG:A mispair.

Table 1. Kinetic, Equilibrium, and Thermodynamic Parameters of G and oxoG Obtained from CLEANEX-PM Spectra^a

Duplex	k_{op} (s ⁻¹)	k'_{cl} (10 ⁴ s ⁻¹)	K'_{eq} (10 ⁻⁶)	T_{m} (K)	ΔH (kJ·mol ⁻¹)	ΔG°_{298} (kJ·mol ⁻¹)	ΔS°_{298} (kJ·mol ⁻¹ ·K ⁻¹)
1	EX2 ^b	EX2	0.158 ± 0.003	340.6 ± 0.2	-466 ± 15	-73.7 ± 1.9	-1.32 ± 0.06
2	EX2	EX2	0.141 ± 0.003	335.7 ± 0.4	-491 ± 22	-70.5 ± 2.5	-1.41 ± 0.08
4	182.7 ± 17.1	31.85 ± 3.14	573.6 ± 17.9	331.1 ± 0.3	-478 ± 19	-63.2 ± 1.9	-1.39 ± 0.07
5	EX2	EX2	0.118 ± 0.009	336.9 ± 0.4	-556 ± 30	-79.6 ± 3.5	-1.60 ± 0.11
6	EX2	EX2	0.048 ± 0.003	336.4 ± 0.3	-575 ± 33	-81.0 ± 3.8	-1.66 ± 0.12
8	75.6 ± 5.1	7.00 ± 0.75	1080 ± 89	329.6 ± 0.4	-565 ± 41	-69.6 ± 4.0	-1.66 ± 0.15

^aFor duplexes 3 and 7, imino protons were not identified, and complex temperature profiles of the ¹H signal prevented determination of melting parameters. ^bEX2, individual constants cannot be determined because the closing rate greatly exceeds the exchange rate.

As calorimetry-based studies indicate DNA destabilization by oxoG:C,¹³ we have tracked temperature dependences of the chemical shift of nonexchangeable thymine methyl protons in our duplexes.³⁶ Both T₃ and T₆/T₉ showed two well-resolved ¹H signals in the characteristic 1–2 ppm region, one of which was used to extract thermodynamic parameters from a two-state model³⁷ (Figure 3, Supporting Information Figures S12,

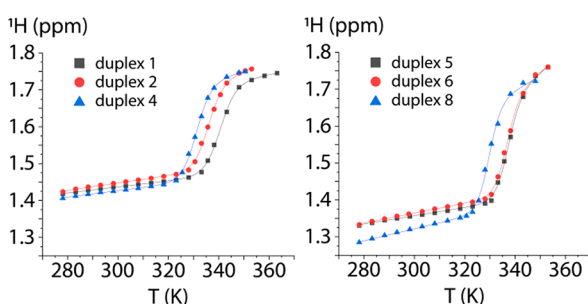


Figure 3. Temperature dependences of the chemical shifts of thymine methyl protons for poorly stacking (left) and well-stacking (right) contexts. Curves, data fitting by eq S13.

S13, Supporting Information Text). Generally, the results were consistent with the calorimetric data: oxoG slightly decreased T_{m} of Watson–Crick duplexes, while the Hoogsteen duplexes were even less stable (Figure 3, Table 1). However, the difference between G:C and oxoG:C in the well-stacking context (5 vs 6) was negligible. Interestingly, ΔH in poorly stacking (1, 2, 4) and well-stacking (5, 6, 8) duplexes closely coincided within each group and differed by ~ 90 kJ·mol⁻¹ between the groups. Since the calorimetric study¹³ employed a poorly stacking C[G/oxoG]C context, it appears that oxoG:C is not always destabilizing. Consistent with the imino proton exchange data and the expected instability of G:A mismatches, duplexes 3 and 7 showed complex temperature dependences of ¹H lines preventing straightforward extraction of thermodynamic parameters.

Overall, our data indicate that the destabilizing effect of oxoG:C in poorly stacking contexts cannot be explained by easier opening of the damaged base pair. However, in duplex 2, the equilibria of base pairs neighboring the damaged ones (G₆ and T₉) are shifted toward the open state in comparison with the undamaged duplex 1, while the near-terminal base pairs (G₂ and T₃) behave similarly in both duplexes (Supporting Information Table S1). We surmise that subtle conformational changes in the oxoG:C pair, such as the BI → BII backbone shift relieving the O⁸–OS' collision,⁸ could spread over the adjacent nucleotides and facilitate their opening, which destabilizes the whole duplex. In the well-stacking context, oxoG:C was not destabilizing, indicating that stacking

compensates for the penalty associated with the O⁸ substituent. Indeed, an extended π -system of oxoG might improve stacking compared with regular purines. Damaged base pairs in our duplexes were separated by only two normal pairs, which may allow some dynamic coupling between the lesions. However, in a molecular dynamic study of G:A in several sequence contexts¹⁰ this mismatch affected the duplex conformation mostly over positions ± 1 with minor disturbances at ± 2 and almost none beyond. Since G:A is the least stable of the mismatches we have analyzed, the distance effect of the others might be even more limited.

Our results may have implications for the mechanism of oxoG search by DNA glycosylases. It is unlikely that oxoG paired with C is captured when extrahelical, since it appears even more stable than G inside the helix. Thus, OGG1 and Fpg would have to enforce oxoG flipout into the active site. In contrast, oxoG is much more available extrahelically when mispaired with A. This observation may relieve contradictions between the biochemical and structural data for MutY: while in all crystal structures oxoG is intrahelical, fast kinetics and cross-linking studies support extrahelical recognition.³⁸ The rate and equilibrium constants for oxoG:A (Table 1, duplexes 4 and 8) can be compared with those measured with DFEA for T and U, for which extrahelical capture by UNG is suggested: $k_{\text{op}} = 35$ s⁻¹, $k'_{\text{cl}} = 180 \times 10^4$ s⁻¹, $K'_{\text{eq}} = 20 \times 10^{-6}$ for T:A, $k_{\text{op}} = 200$ s⁻¹, $k'_{\text{cl}} = 700 \times 10^4$ s⁻¹, $K'_{\text{eq}} = 27 \times 10^{-6}$ for U:A, and $k_{\text{op}} = 650$ s⁻¹, $k'_{\text{cl}} = 130 \times 10^4$ s⁻¹, $K'_{\text{eq}} = 500 \times 10^{-6}$ for T:6-methylpurine (a pair with only one hydrogen bond).^{23,26} Thus, oxoG in oxoG:A is even more accessible extrahelically than a destabilized thymine. We hypothesize that a spontaneously everted oxoG may be captured by MutY/MUTYH as an early substrate recognition step.

ASSOCIATED CONTENT

Supporting Information

The Supporting Information is available free of charge at <https://pubs.acs.org/doi/10.1021/jacs.2c11230>.

Additional experimental details, description of proton exchange formalism and NMR experiments, supplementary discussion, as well as supplementary Tables and Figures including additional experimental results (PDF)

AUTHOR INFORMATION

Corresponding Authors

Elena G. Bagryanskaya – Vorozhtsov Novosibirsk Institute of Organic Chemistry SB RAS, Novosibirsk 630090, Russia;

orcid.org/0000-0003-0057-383X;

Email: egbagryanskaya@nioch.nsc.ru

Dmitry O. Zharkov – Institute of Chemical Biology and Fundamental Medicine SB RAS, Novosibirsk 630090,

Russia; Novosibirsk State University, Novosibirsk 630090, Russia; orcid.org/0000-0001-5013-0194; Email: dzharkov@niboch.nsc.ru

Authors

Sergey S. Ovcherenko – Vorozhtsov Novosibirsk Institute of Organic Chemistry SB RAS, Novosibirsk 630090, Russia; Novosibirsk State University, Novosibirsk 630090, Russia

Andrey V. Shernyukov – Vorozhtsov Novosibirsk Institute of Organic Chemistry SB RAS, Novosibirsk 630090, Russia; orcid.org/0000-0001-7463-7598

Dmitry M. Nasonov – Vorozhtsov Novosibirsk Institute of Organic Chemistry SB RAS, Novosibirsk 630090, Russia; Novosibirsk State University, Novosibirsk 630090, Russia

Anton V. Endutkin – Institute of Chemical Biology and Fundamental Medicine SB RAS, Novosibirsk 630090, Russia

Complete contact information is available at:

<https://pubs.acs.org/10.1021/jacs.2c11230>

Author Contributions

The manuscript was written through contributions of all authors.

Funding

This study was supported by Russian Science Foundation (21-14-00219). Partial salary support from Russian Ministry of Science and Higher Education (12103130005-8) is acknowledged.

Notes

The authors declare no competing financial interest.

ACKNOWLEDGMENTS

We thank Dr. Sergey Smirnov (Western Washington University) for useful discussion and Ms. Tatyana Bushueva for synthesis of oligonucleotides.

ABBREVIATIONS

Fpg, DNA-formamidopyrimidine glycosylase; OGG1, 8-oxoguanine DNA glycosylase; MutY (or human MUTYH), adenine DNA glycosylase; UNG, uracil-DNA glycosylase; dAMP, deoxyadenosine monophosphate

REFERENCES

- (1) von Sonntag, C. *Free-Radical-Induced DNA Damage and Its Repair: A Chemical Perspective*; Springer, 2006. Cadet, J.; Davies, K. J. A.; Medeiros, M. H. G.; Di Mascio, P.; Wagner, J. R. Formation and repair of oxidatively generated damage in cellular DNA. *Free Radic. Biol. Med.* **2017**, *107*, 13–34.
- (2) Dizdaroglu, M.; Coskun, E.; Tuna, G.; Kant, M.; Jaruga, P. Oxidatively induced DNA damage: Mechanisms and measurement. In *DNA Damage, DNA Repair and Disease*; Dizdaroglu, M., Lloyd, R. S., Eds.; Royal Society of Chemistry, 2021; Vol. 1; pp 86–116.
- (3) ESCODD (European Standards Committee on Oxidative DNA Damage); Gedik, C. M.; Collins, A. Establishing the background level of base oxidation in human lymphocyte DNA: Results of an interlaboratory validation study. *FASEB J.* **2005**, *19* (1), 82–84. Poulsen, H. E.; Nadal, L. L.; Broedbaek, K.; Nielsen, P. E.; Weimann, A. Detection and interpretation of 8-oxodG and 8-oxoGua in urine, plasma and cerebrospinal fluid. *Biochim. Biophys. Acta* **2014**, *1840* (2), 801–808.
- (4) Zahn, K. E.; Wallace, S. S.; Doublie, S. DNA polymerases provide a canon of strategies for translesion synthesis past oxidatively generated lesions. *Curr. Opin. Struct. Biol.* **2011**, *21* (3), 358–369.
- (5) Alexandrov, L. B.; Nik-Zainal, S.; Wedge, D. C.; Aparicio, S. A. J. R.; Behjati, S.; Biankin, A. V.; Bignell, G. R.; Bolli, N.; Borg, A.;

Borresen-Dale, A.-L.; et al. Signatures of mutational processes in human cancer. *Nature* **2013**, *500* (7463), 415–421. Viel, A.; Bruselles, A.; Meccia, E.; Fornasari, M.; Quaia, M.; Canzonieri, V.; Policicchio, E.; Urso, E. D.; Agostini, M.; Genuardi, M.; et al. A specific mutational signature associated with DNA 8-oxoguanine persistence in MUTYH-defective colorectal cancer. *EBioMedicine* **2017**, *20*, 39–49.

(6) Cho, B. P.; Kadlubar, F. F.; Culp, S. J.; Evans, F. E. ¹⁵N nuclear magnetic resonance studies on the tautomerism of 8-hydroxy-2'-deoxyguanosine, 8-hydroxyguanosine, and other C8-substituted guanine nucleosides. *Chem. Res. Toxicol.* **1990**, *3* (5), 445–452.

(7) Oda, Y.; Uesugi, S.; Ikehara, M.; Nishimura, S.; Kawase, Y.; Ishikawa, H.; Inoue, H.; Ohtsuka, E. NMR studies of a DNA containing 8-hydroxydeoxyguanosine. *Nucleic Acids Res.* **1991**, *19* (7), 1407–1412. Lipscomb, L. A.; Peek, M. E.; Morningstar, M. L.; Verghis, S. M.; Miller, E. M.; Rich, A.; Essigmann, J. M.; Williams, L. D. X-ray structure of a DNA decamer containing 7,8-dihydro-8-oxoguanine. *Proc. Natl. Acad. Sci. U.S.A.* **1995**, *92* (3), 719–723.

(8) Hoppins, J. J.; Gruber, D. R.; Miers, H. L.; Kiryutin, A. S.; Kasymov, R. D.; Petrova, D. V.; Endutkin, A. V.; Popov, A. V.; Yurkovskaya, A. V.; Fedechkin, S. O.; et al. 8-Oxoguanine affects DNA backbone conformation in the EcoRI recognition site and inhibits its cleavage by the enzyme. *PLoS One* **2016**, *11*, No. e0164424. Gruber, D. R.; Toner, J. J.; Miers, H. L.; Shernyukov, A. V.; Kiryutin, A. S.; Lomzov, A. A.; Endutkin, A. V.; Grin, I. R.; Petrova, D. V.; Kupryushkin, M. S.; et al. Oxidative damage to epigenetically methylated sites affects DNA stability, dynamics, and enzymatic demethylation. *Nucleic Acids Res.* **2018**, *46* (20), 10827–10839.

(9) Kouchakdjian, M.; Bodepudi, V.; Shibutani, S.; Eisenberg, M.; Johnson, F.; Grollman, A. P.; Patel, D. J. NMR structural studies of the ionizing radiation adduct 7-hydro-8-oxodeoxyguanosine (8-oxo-7H-dG) opposite deoxyadenosine in a DNA duplex. 8-Oxo-7H-dG(syn)•dA(anti) alignment at lesion site. *Biochemistry* **1991**, *30* (5), 1403–1412. Gannett, P. M.; Sura, T. P. Base pairing of 8-oxoguanosine and 8-oxo-2'-deoxyguanosine with 2'-deoxyadenosine, 2'-deoxycytosine, 2'-deoxyguanosine, and thymidine. *Chem. Res. Toxicol.* **1993**, *6* (5), 690–700.

(10) Rossetti, G.; Dans, P. D.; Gomez-Pinto, I.; Ivani, I.; Gonzalez, C.; Orozco, M. The structural impact of DNA mismatches. *Nucleic acids research* **2015**, *43* (8), 4309–4321.

(11) Sanchez, A. M.; Volk, D. E.; Gorenstein, D. G.; Lloyd, R. S. Initiation of repair of A/G mismatches is modulated by sequence context. *DNA repair* **2003**, *2* (8), 863–878. Hunter, W. N.; Brown, T.; Kennard, O. Structural features and hydration of d(C-G-C-G-A-A-T-T-A-G-C-G); a double helix containing two G.A mispairs. *J. Biomol. Struct. Dyn.* **1986**, *4* (2), 173–191. Kan, L. S.; Chandrasegaran, S.; Pulford, S. M.; Miller, P. S. Detection of a guanine X adenine base pair in a decaoxyribonucleotide by proton magnetic resonance spectroscopy. *Proc. Natl. Acad. Sci. U. S. A.* **1983**, *80* (14), 4263–4265.

(12) Cheng, X.; Kelso, C.; Hornak, V.; de los Santos, C.; Grollman, A. P.; Simmerling, C. Dynamic behavior of DNA base pairs containing 8-oxoguanine. *J. Am. Chem. Soc.* **2005**, *127* (40), 13906–13918.

(13) Plum, G. E.; Grollman, A. P.; Johnson, F.; Breslauer, K. J. Influence of the oxidatively damaged adduct 8-oxodeoxyguanosine on the conformation, energetics, and thermodynamic stability of a DNA duplex. *Biochemistry* **1995**, *34* (49), 16148–16160.

(14) Miller, J. H.; Fan-Chiang, C.-C. P.; Straatsma, T. P.; Kennedy, M. A. 8-Oxoguanine enhances bending of DNA that favors binding to glycosylases. *J. Am. Chem. Soc.* **2003**, *125* (20), 6331–6336.

(15) Barone, F.; Lankas, F.; Spackova, N.; Sponer, J.; Karran, P.; Bignami, M.; Mazzei, F. Structural and dynamic effects of single 7-hydro-8-oxoguanine bases located in a frameshift target DNA sequence. *Biophys. Chem.* **2005**, *118* (1), 31–41.

(16) Boiteux, S.; Coste, F.; Castaing, B. Repair of 8-oxo-7,8-dihydroguanine in prokaryotic and eukaryotic cells: Properties and biological roles of the Fpg and OGG1 DNA N-glycosylases. *Free Radic. Biol. Med.* **2017**, *107*, 179–201. Yudkina, A. V.; Shilkin, E. S.; Endutkin, A. V.; Makarova, A. V.; Zharkov, D. O. Reading and

misreading 8-oxoguanine, a paradigmatic ambiguous nucleobase. *Crystals* **2019**, *9*, 269.

(17) Bruner, S. D.; Norman, D. P. G.; Verdine, G. L. Structural basis for recognition and repair of the endogenous mutagen 8-oxoguanine in DNA. *Nature* **2000**, *403* (6772), 859–866.

(18) Gilboa, R.; Zharkov, D. O.; Golan, G.; Fernandes, A. S.; Gerchman, S. E.; Matz, E.; Kycia, J. H.; Grollman, A. P.; Shoham, G. Structure of formamidopyrimidine-DNA glycosylase covalently complexed to DNA. *J. Biol. Chem.* **2002**, *277* (22), 19811–19816.

(19) Fromme, J. C.; Verdine, G. L. DNA lesion recognition by the bacterial repair enzyme MutM. *J. Biol. Chem.* **2003**, *278* (51), 51543–51548. Banerjee, A.; Yang, W.; Karplus, M.; Verdine, G. L. Structure of a repair enzyme interrogating undamaged DNA elucidates recognition of damaged DNA. *Nature* **2005**, *434* (7033), 612–618. Banerjee, A.; Verdine, G. L. A nucleobase lesion remodels the interaction of its normal neighbor in a DNA glycosylase complex. *Proc. Natl. Acad. Sci. U.S.A.* **2006**, *103* (41), 15020–15025. Kuznetsov, N. A.; Koval, V. V.; Zharkov, D. O.; Vorobjev, Y. N.; Nevinsky, G. A.; Douglas, K. T.; Fedorova, O. S. Pre-steady-state kinetic study of substrate specificity of *Escherichia coli* formamidopyrimidine-DNA glycosylase. *Biochemistry* **2007**, *46* (2), 424–435. Kuznetsov, N. A.; Koval, V. V.; Nevinsky, G. A.; Douglas, K. T.; Zharkov, D. O.; Fedorova, O. S. Kinetic conformational analysis of human 8-oxoguanine-DNA glycosylase. *J. Biol. Chem.* **2007**, *282* (2), 1029–1038. Qi, Y.; Spong, M. C.; Nam, K.; Banerjee, A.; Jiralerspong, S.; Karplus, M.; Verdine, G. L. Encounter and extrusion of an intrahelical lesion by a DNA repair enzyme. *Nature* **2009**, *462* (7274), 762–766. Li, H.; Endutkin, A. V.; Bergonzo, C.; Campbell, A. J.; de los Santos, C.; Grollman, A.; Zharkov, D. O.; Simmerling, C. A dynamic checkpoint in oxidative lesion discrimination by formamidopyrimidine-DNA glycosylase. *Nucleic Acids Res.* **2016**, *44* (2), 683–694. Li, H.; Endutkin, A. V.; Bergonzo, C.; Fu, L.; Grollman, A. P.; Zharkov, D. O.; Simmerling, C. DNA deformation-coupled recognition of 8-oxoguanine: Conformational kinetic gating in human DNA glycosylase. *J. Am. Chem. Soc.* **2017**, *139* (7), 2682–2692. Shigdel, U. K.; Ovchinnikov, V.; Lee, S.-J.; Shih, J. A.; Karplus, M.; Nam, K.; Verdine, G. L. The trajectory of intrahelical lesion recognition and extrusion by the human 8-oxoguanine DNA glycosylase. *Nat. Commun.* **2020**, *11*, 4437.

(20) Banerjee, A.; Santos, W. L.; Verdine, G. L. Structure of a DNA glycosylase searching for lesions. *Science* **2006**, *311* (5764), 1153–1157. Kuznetsov, N. A.; Bergonzo, C.; Campbell, A. J.; Li, H.; Mechetin, G. V.; de los Santos, C.; Grollman, A. P.; Fedorova, O. S.; Zharkov, D. O.; Simmerling, C. Active destabilization of base pairs by a DNA glycosylase wedge initiates damage recognition. *Nucleic Acids Res.* **2015**, *43* (1), 272–281.

(21) Sung, R.-J.; Zhang, M.; Qi, Y.; Verdine, G. L. Structural and biochemical analysis of DNA helix invasion by the bacterial 8-oxoguanine DNA glycosylase MutM. *J. Biol. Chem.* **2013**, *288* (14), 10012–10023.

(22) Cao, C.; Jiang, Y. L.; Stivers, J. T.; Song, F. Dynamic opening of DNA during the enzymatic search for a damaged base. *Nat. Struct. Mol. Biol.* **2004**, *11* (12), 1230–1236.

(23) Cao, C.; Jiang, Y. L.; Krosky, D. J.; Stivers, J. T. The catalytic power of uracil DNA glycosylase in the opening of thymine base pairs. *J. Am. Chem. Soc.* **2006**, *128* (40), 13034–13035.

(24) Parker, J. B.; Bianchet, M. A.; Krosky, D. J.; Friedman, J. I.; Amzel, L. M.; Stivers, J. T. Enzymatic capture of an extrahelical thymine in the search for uracil in DNA. *Nature* **2007**, *449* (7161), 433–437. Friedman, J. I.; Majumdar, A.; Stivers, J. T. Nontarget DNA binding shapes the dynamic landscape for enzymatic recognition of DNA damage. *Nucleic Acids Res.* **2009**, *37* (11), 3493–3500.

(25) Every, A. E.; Russu, I. M. Opening dynamics of 8-oxoguanine in DNA. *Journal of Molecular Recognition* **2013**, *26* (4), 175–180. Crenshaw, C. M.; Wade, J. E.; Arthanari, H.; Frueh, D.; Lane, B. F.; Núñez, M. E. Hidden in plain sight: subtle effects of the 8-oxoguanine lesion on the structure, dynamics, and thermodynamics of a 15-base pair oligodeoxynucleotide duplex. *Biochemistry* **2011**, *50* (39), 8463–8477.

(26) Parker, J. B.; Stivers, J. T. Dynamics of uracil and 5-fluorouracil in DNA. *Biochemistry* **2011**, *50* (5), 612–617.

(27) Yin, Y.; Yang, L.; Zheng, G.; Gu, C.; Yi, C.; He, C.; Gao, Y. Q.; Zhao, X. S. Dynamics of spontaneous flipping of a mismatched base in DNA duplex. *Proc. Natl. Acad. Sci. U. S. A.* **2014**, *111* (22), 8043–8048. Banavali, N. K.; MacKerell, A. D., Jr Free energy and structural pathways of base flipping in a DNA GCGC containing sequence. *Journal of molecular biology* **2002**, *319* (1), 141–160. Várnai, P.; Canalia, M.; Leroy, J. L. Opening mechanism of G.T/U pairs in DNA and RNA duplexes: a combined study of imino proton exchange and molecular dynamics simulation. *J. Am. Chem. Soc.* **2004**, *126* (44), 14659–14667.

(28) Mori, S.; Johnson, M. O.; Berg, J. M.; van Zijl, P. C. M. Water exchange filter (WEX filter) for nuclear magnetic resonance studies of macromolecules. *J. Am. Chem. Soc.* **1994**, *116* (26), 11982–11984.

(29) Mori, S.; Abeygunawardana, C.; van Zijl, P. C. M.; Berg, J. M. Water exchange filter with improved sensitivity (WEX II) to study solvent-exchangeable protons. Application to the consensus zinc finger peptide CP-1. *J. Magn. Reson. B* **1996**, *110* (1), 96–101.

(30) Gemmecker, G.; Jahnke, W.; Kessler, H. Measurement of fast proton exchange rates in isotopically labeled compounds. *J. Am. Chem. Soc.* **1993**, *115* (24), 11620–11621.

(31) Macura, S.; Wüthrich, K.; Ernst, R. R. Separation and suppression of coherent transfer effects in two-dimensional NOE and chemical exchange spectroscopy. *J. Magn. Reson.* **1982**, *46* (2), 269–282.

(32) Hwang, T.-L.; Mori, S.; Shaka, A. J.; van Zijl, P. C. M. Application of Phase-Modulated CLEAN chemical EXchange spectroscopy (CLEANEX-PM) to detect water–protein proton exchange and intermolecular NOEs. *J. Am. Chem. Soc.* **1997**, *119* (26), 6203–6204. Hwang, T.-L.; van Zijl, P. C. M.; Mori, S. Accurate quantitation of water-amide proton exchange rates using the phase-modulated CLEAN chemical EXchange (CLEANEX-PM) approach with a Fast-HSQC (FHSQC) detection scheme. *J. Biomol. NMR* **1998**, *11* (2), 221–226.

(33) von Hippel, P. H.; Johnson, N. P.; Marcus, A. H. Fifty years of DNA “breathing”: Reflections on old and new approaches. *Biopolymers* **2013**, *99* (12), 923–954.

(34) Pyshnyi, D. V.; Goldberg, E. L.; Ivanova, E. M. Efficiency of coaxial stacking depends on the DNA duplex structure. *J. Biomol. Struct. Dyn.* **2003**, *21* (3), 459–467.

(35) Guéron, M.; Leroy, J.-L. Studies of base pair kinetics by NMR measurement of proton exchange. *Methods Enzymol.* **1995**, *261*, 383–413.

(36) Taylor, J.-S.; Garrett, D. S.; Brockie, I. R.; Svoboda, D. L.; Telsler, J. ¹H NMR assignment and melting temperature study of cis-syn and trans-syn thymine dimer containing duplexes of d-(CGTATTATGC)•d(GCATAATACG). *Biochemistry* **1990**, *29* (37), 8858–8866.

(37) Marky, L. A.; Breslauer, K. J. Calculating thermodynamic data for transitions of any molecularity from equilibrium melting curves. *Biopolymers* **1987**, *26* (9), 1601–1620.

(38) Hickerson, R. P.; Chepanoske, C. L.; Williams, S. D.; David, S. S.; Burrows, C. J. Mechanism-based DNA-protein cross-linking of MutY via oxidation of 8-oxoguanosine. *J. Am. Chem. Soc.* **1999**, *121* (42), 9901–9902. Bernards, A. S.; Miller, J. K.; Bao, K. K.; Wong, I. Flipping duplex DNA inside out: A double base-flipping reaction mechanism by *Escherichia coli* MutY adenine glycosylase. *J. Biol. Chem.* **2002**, *277* (23), 20960–20964.